Impermeable thin Al_2O_3 overlay for TBC protection from sulfate and vanadate attack in gas turbines

Quarterly Progress Report

Reporting Period Start Date: Apr. 1, 2004
Reporting Period End Date: June 30, 2004
Principal Author: Scott X. Mao
Date Report was issued (June 30, 2004)
DOE Award Number: DE-FC26-01NT41189

Department of Mechanical Engineering
University of Pittsburgh
3700 O'Hara St.
Pittsburgh, PA 15261
smao@engrng.pitt.edu, Tel: 412-624-9282

DISCLAIMER

ABSTRACT

In order to further improve the hot corrosion resistance of yttria-stabilized zirconia (YSZ), an Al_2O_3 overlay of 58 *mm* thick was deposited on the surface of YSZ by electron-beam physical vapor deposition. Hot corrosion tests were performed on the YSZ coatings with γ-Al_2O_3 overlay and α-Al_2O_3 overlay in molten salt mixture (Na_2SO_4 + 5wt%V_2O_5) at 950^{o}C. The α-Al_2O_3 overlay was obtained by the post-annealing of γ-Al_2O_3 overlay at 1200^{o}C for 1h.The results showed that compared with the hot corrosion resistance of YSZ coating with 25 *mm* thick γ-Al_2O_3 overlay, either thickening γ-Al_2O_3 overlay or employing α-Al_2O_3 overlay could impair the hot corrosion resistance of YSZ coating, because the tensile stresses developed in the alumina overlay in both cases due to the mismatch in thermal expansion coefficient (TEC) between alumina and zirconia resulted in cracking of Al_2O_3 overlay. The formation of cracks increased contact area between molten salt and Al_2O_3 overlay, and also the penetration rate of molten salt into Al_2O_3 overlay and YSZ coating, leading a faster and greater degradation of YSZ coating upon exposure.

In the next reporting period, we will study the effect of Al_2O_3 overlay thickness on hot corrosion and spalling of YSZ coatings.

TABLE OF CONTENTS

LIST OF GRAPHICAL MATERIALS

1. INTRODUCTION

Thermal-barrier coatings (TBCs), which consist of an yttria stabilized zirconia (YSZ) top-coating and an intermediate MCrAlY (M=Ni, Co, Fe) bond coating, are extensively used in gas turbines.[1-5] The application of TBCs can improve the durability of components and enhance the engine efficiency by increasing the turbine inlet combustion temperature. The common failure mode of TBC used in aviation gas turbines is that a thermally-growth oxide (TGO) forms and continuously grows between the top-coating and the bond coat. Because of the thermal expansion mismatch between the TGO and the bond coat, thermal cycling results in cracking, even spalling of TBCs.

TBCs are also finding increasing application in land-based industrial engines and sea engines which are usually operated with low quality fuels containing sulfur and vanadium.[5] In this case, another failure mode — hot corrosion become predominant and crucial to the lifetime of TBCs. During service, molten sulfate and vanadate salt condense on the TBCs at the temperature of 600-1000°C.[6, 7] Although zirconia itself shows good resistance to the attack of the molten sulfate or vanadate compounds arising from fuel impurities, yttria is leached out of the zirconia by the reaction with V_2O_5 or $NaVO_3$ to form YVO_4, causing the structural

destabilization of ZrO_2 (*i.e.*, transformation of the zirconia from the tetragonal and/or cubic to monoclinic phase). The structural destabilization of ZrO_2 is accompanied by a large destructive volume change, leading to large stresses within the YSZ, which eventually results in the delamination and spalling of the coating.[8-13]

Further improvement of engine efficiency requires TBCs being an integral part of the component which, in turn, desires reliable and predictable TBC performance. Hence, many methods have been developed to improve the hot corrosion resistant of TBCs to such harsh environment containing sulfate-vanadate deposits. For instance, based on Lewis acid-base concept, zirconias stabilized with india (In_2O_3),[14,15] scandia (Sc_2O_3)[16] and ceria (CeO_2)[11,17] as well as Ta_2O_5 [9, 18] and $YTaO_4$[18] have been evaluated for their hot corrosion resistance. On the other hand, over the years attempt has been made to seal the surface of zirconia TBCs by laser-glazing and arc lamp[19-21] or various "seal coats"[21-25] to prevent the penetration of molten deposits into the porous YSZ coating.

Our previous results have shown that Al_2O_3 overlay acted as a barrier layer against the infiltration of the molten salt into the YSZ coating during exposure to the molten salt containing VO. However, Al_2O_3 overlay could be degraded by the formation of low-melting Na_2O-V_2O_5-Al_2O_3 liquid phase. In the present work, the thickness of electron-beam physical vapor deposited high-purity Al_2O_3 overlay was increased to 58μm to investigate whether a thick Al_2O_3 overlay can further improve the hot corrosion resistance of TBC. The composite YSZ/Al_2O_3 system will be exposed to the molten salt (Na_2SO_4+ 5wt%V_2O_5) at 950°C.

2. EXECUTIVE SUMMARY

Compared with the hot corrosion resistance of YSZ coating with 25 *mm* thick γ-Al_2O_3 overlay, either thickening γ-Al_2O_3 overlay or employing α-Al_2O_3 overlay could impair the hot corrosion resistance of YSZ coating.

3. EXPERIMENTAL

The TBC system used in the present work consisted of 6061 nickel-based superalloy substrate, CoNiCrAlY alloy bond coat as well as zirconia-8wt%yttira (YSZ) ceramic top coating. The 100 μm thick bond coating and the 200 μm thick YSZ were produced by low-pressure plasma spray (LPPS) and air plasma spray (APS), respectively.

The Al_2O_3 overlay was deposited by EB-PVD. The aluminum oxide coatings were deposited using an EB-PVD unit. Prior to deposition, the 1.5"x1.5" coupons were ultrasonically cleaned and dried. The vacuum unit was pumped down to a base pressure of 7.5 x 10^{-6} Torr with the oxygen gas lines being evacuated. Using two of the electron beams, the samples were preheated to ~1000°C and allowed to soak at 1000 °C for 20 minutes. During the evaporation of aluminum oxide, ~150 sccm of oxygen was flowed into the chamber to maintain the oxygen stoichiometry of the condensing coating (chamber pressure ~ 1x10^{-3} Torr). The average condensation rate was 0.88 μm/min. At the end of the desired deposition time, the samples were retracted into the load lock chamber and allowed to cool for 10 minutes with ~200 sccm of

oxygen flow of before venting to atmosphere. The thickness of Al_2O_3 coating was approximately 58 μm.

Hot corrosion test was carried out on the TBCs with and without Al_2O_3 coating. The TBC plates were coated with a 150 mg cm^{-2} salt mixture (Na_2SO_4 + 5wt%V_2O_5) on a hot plate by dipping in a aqueous slurry of salt (1000 g / *l*), then placed carefully into a still air furnace, and isothermally held at 950°C for 10 hours. Melting of the salts mixture produced a thin liquid film on the surface of specimens. After exposure, the specimens were cooled down to room temperature in the furnace. The exposed specimens were cleaned in de-ionized water, resined in isoprypol alcohol and then dried. The Philips PW1700 X-ray diffractometer was then employed to analyze the corrosion products and phase transformation of ZrO_2 ceramic in the exposed samples.

The microstructure, composition of the coating surface and the cross-section were also examined using the PHILIPS XL30 scanning electron microscope (FE-SEM) equipped with an energy-dispersive spectrometer (EDS).

4. RESULTS AND DISCUSSION

4.1 XRD measurement

Consist with the previous results, the as-deposited Al_2O_3 overlay showed the γ-phase structure. Fig.1 shows the XRD patterns of the composite YSZ/Al_2O_3 system after hot corrosion testing. It can be seen that the γ-Al_2O_3 phase was transformed to α-Al_2O_3 phase after exposure to the mixed molten salt of Na_2SO_4+5wt.%V_2O_5 (Pattern A in Fig.1). When part of Al_2O_3 overlay was removed, the formation M-phase of ZrO_2 in the YSZ coating was evident (Pattern B in Fig.1). The results also showed that no YVO_4 peaks were present due to its low content that was below the detection limit of the XRD. The T-phase of ZrO_2 in the YSZ coating was still predominant. To investigate whether the α-Al_2O_3 overlay has better corrosion resistant than the γ-Al_2O_3 phase, the composite YSZ/Al_2O_3 system was heated at 1200°C for 1 hour in air before hot corrosion, which leads to transformation of γ-Al_2O_3 to α-Al_2O_3 phase (Pattern A in Fig.2). Pattern B in Fig.2 shows XRD pattern of TBC with α-Al_2O_3 overlay after exposure to Na_2SO_4+5wt.%V_2O_5.

In order to evaluate the hot corrosion resistance of the TBCs with and without Al_2O_3 overlay, the extent of destabilization (*D*) of zirconia was estimated by

$$\mathrm{D}\ (\%) = \frac{M}{T+M} \times 100 \qquad (1)$$

Where *T* is the intensity of the zirconia tetragonal (111) peak, and *M* is the intensity of the ZrO_2 monoclinic $(11\bar{1})$ peak in XRD tests. Figure 3 shows the destabilization fraction of ZrO_2 (*D*%) after exposure to molten salts at 950°C for 10h. It can be seen from Fig.3 that both the YSZ with γ-Al_2O_3 overlay and YSZ with α-Al_2O_3 overlay improved hot corrosion resistant of monolithic YSZ coating. However, the hot corrosion resistant of YSZ with either a thicker γ-Al_2O_3 overlay or a α-Al_2O_3 overlay was not as good as YSZ with 25 μm γ-Al_2O_3 overlay.

4.2 SEM observation

Fig.4 shows the cross-section SEM images of YSZ with γ-Al_2O_3 overlay before and after exposure to the molten salt. It can be seen that the γ-Al_2O_3 overlay was intimately contacted with YSZ coating before exposure, but grooves existed within the overlay. After exposure, coarse acicular-shape α-Al_2O_3 crystals and faceted crystals were present and the Al_2O_3 overlay became very loose, especially adjacent to the YSZ coating.

After hot corrosion testing, EDS analysis was performed on cross-section of TBC coating as shown in Fig.5. The Al Kα-dot map exhibited evidently that the Al_2O_3 overlay was no long dense and well contacted to the YSZ coating. In addition, S, Na, and V can be detected at the Al_2O_3 overlay-YSZ interface and also within the Al_2O_3 overlay and YSZ coating. These results indicated that the molten salt containing V_2O_5 and Na_2O covered the surface of the Al_2O_3 overlay was infiltrated along the grooves to the interface between Al_2O_3 overlay and YSZ coating. As a result, the coexistence of V_2O_5, Na_2O and Al_2O_3 led to the formation of low-melting liquid phase of Na_2O-V_2O_5-Al_2O_3. The continuous formation of the liquid phase can result in loss of integrity of the surface and inner alumina. At the same time, the low-melting liquid phase penetrated into pores and cracks within the YSZ coating, leading to the reaction occurs between V_2O_5 and YSZ to form YVO_4 and hence the formation of M-phase ZrO_2.

Compared with the hot corrosion results of YSZ with 25 *mm* γ-Al_2O_3 overlay, more M-phase ZrO_2 formation in the case of YSZ with 58 *mm* γ-Al_2O_3 overlay was probably due to the thicker γ-Al_2O_3 overlay was easy to crack during exposure because the heating cycle causes tensile stresses in the alumina due to the mismatch in thermal expansion coefficient (TEC) between alumina (TEC $\approx 8-9\times10^{-6}/^{o}C$) and zirconia (TEC $\approx 11-13\times10^{-6}/^{o}C$). The formation of cracks increased contact area between molten salt and Al_2O_3 overlay, and also increased the penetration rate of molten salt into Al_2O_3 overlay and YSZ coating.

Fig.6 demonstrates the SEM cross-section images of YSZ with 58 *mm* γ-Al_2O_3 overlay after heat treatment at $1200^{o}C$ in air and followed by exposure to the molten salt. Fig.7 shows EDS analysis performed on cross-section of TBC coating exposured to the molten salt after heat treatment. It is clearly seen that many cracks had been formed from original groove within the α-Al_2O_3 overlay after heat treatment. Upon exposure to the molten salt, although the α-Al_2O_3 overlay showed much less dissolution in molten salt, the molten salt could easily penetrate into YSZ coating through the cracks, as evidenced by the presence of Na, S, and V within the YSZ coating, leading to the degradation of YSZ coating.

5. PLANS FOR THE NEXT REPORTING PERIOD

In the next reporting period, we will study the effect of Al_2O_3 overlay thickness on hot corrosion and spalling of YSZ coatings.

6. CONCLUSION

(1) Dissolution of Al_2O_3 in molten $NaVO_3$ was responsible for degradation of the Al_2O_3 overlay during hot corrosion testing. Degradation of the Al_2O_3 overlay was deteriorated with increase in its thickness.
(2) The formation of cracks in α-Al_2O_3 overlay led faster and more degradation of the YSZ coating, although the α-Al_2O_3 overlay showed much less dissolution in molten salt.

7. REFERENCES

[1] M. J. Stiger, N. M. Yanar, M. G. Topping, F. S. Pettit, and G. H. Meier, "Thermal barrier coatings for the 21st century," *Z. Metallkd*, **90**[12] 1069-1078 (1999).

[2] L. Singheiser, R. Steinbrech, W.J. Quadakkers, R. Herzog, "Failure aspects of thermal barrier coatings", *Mat. High Temp*, **18** [4] 249-259 (2001)

[3] I. Gurrappa, "Hot corrosion of protective coatings," *Mat. Manuf. Process*, **15** [5]: 761-773 (2000).

[4] I. Gurrappa, "Thermal barrier coating for hot corrosion resistance of CM 247 LC superalloy," *J. Mater. Sci. Lett*. **17**, 1267-1269 (1998).

[5] R L. Jones, "Thermogravimetric study of the 800 degree reaction of zirconia stabilizing oxides with SO_3-$NaVO_3$," *J. Electrochem. Soc*., **139**, 2794-2799 (1992).

[6] K. L. Luthra, H. S. Spacil, "Impurity deposits in gas-turbines from fuels containing sodium and vanadium ," *J. Electrochem. Soc*., **129**[3] 649-656 (1982).

[7] N. S. Bornstein and W. P. Allen, "The chemistry of sulfidation corrosion - Revisited," *Mater. Sci. Forum*, **127,** 251-254 (1997).

[8] A. S. Nagelberg, "Destabilization of yttria-stabilized zirconia induced by molten sodium vanadate-sodium sulfate melts," *J. Electrochem. Soc.*, **132**[10] 2502-2507 (1985).

[9] R. L. Jones, C. E. Williams and S. R. Jones, "Reaction of vanadium compounds with ceramic oxides," *J. Electrochem. Soc.*, **133**[1] 227-230 (1986).

[10] R L. Jones, "High temperature vanadate corrosion of yttria-stabilized zirconia coatings on mild steel," *Surf. Coat. Tech.*, **37**, 271-284 (1989).

[11] R. L. Jones and C. E. Williams, "Hot corrosion studies of zirconia ceramics," *Surf. Coat. Tech.*, **32**, 349-358 (1987).

[12] D. W. Susnitzky, W. Hertl and C. B Carter, "Destabilization of zirconia thermal barriers in the presence of V_2O_5," *J. Am. Ceram. Soc*., **71**[11] 992-1004 (1988).

[13] R. A. Miller and C E. Lowell, "Failure mechanism of thermal barrier coatings exposed to elevated temperature," *Thin solid films*, **95**, 265-273 (1982).

[14] R. L. Jones, "India as a hot corrosion-resistant stabilizer for zirconia," *J. Am. Ceram. Soc*., **75** 1818-1821 (1992).

[15] R. L. Jones and R. F. Reidy, "Vanadate hot corrosion behavior of India, yttria-stabilized zirconia," *J. Am. Ceram. Soc*., **76**[10] 2660-2662 (1993).

[16] R. L. Jones, "Scandia-stabilized zirconia for resistance to molten vanadate-sulfate corrosion," *Surf. Coat. Tech.*, **39/40**, 89-96 (1989).

[17] S. A. Muqtader, R. K. Sidhu, E. Nagabhushan, K. Muzaffaruddin and S. G. Samdani, "Destabilization behavior of ceria-stabilized tetragonal zirconia polycrystals by sodium sulphate and vanadium oxide melts," *J. Mater .Sci. Lett*., **12**, 831-833 (1993).
[18] S. Raghavan and M J. Mayo, "The hot corrosion resistance of 20 mol% $YTaO_4$ stabilized tetragonal zirconia and 14 mol% Ta_2O_5 stabilized orthorhombic zirconia for thermal barrier coating applications," *Surf. Coat. Tech.,* **160**, 187-196 (2002).
[19] A. Petitbon, L. Boquet and D. Delsart, "Laser surface sealing and strengthening of zirconia coatings," *Surf. Coat. Tech.,* **49**, 57-61 (1991).
[20] Z. Liu, "Crack-free surface sealing of plasma sprayed ceramic coating using an excimer laser," *Appl. Surf. Sci.*, **186**, 135-139 (2002).
[21] S. Ahmaniemi, P. Vuoristo and T. Mantyla, "Improved sealing treatment for thick thermal barrier coatings," *Surf. Coat. Tech.,* **151-152**, 412-417 (2002).
[22] T. Mantyla, P. Vuoristo and P. Kettunen, "Chemical vapor deposition densification of plasma-sprayed oxide coatings," *Thin solid films,* **118**, 437-444 (1984).
[23] I. Berezin and T. Troczynski, "Surface modification of zirconia thermal barrier coatings," *J. Mater. Sci. Lett*., **15**, 214-218 (1996).
[24] T. Troczynski, Q. Yang and G. John, "Post-deposition treatment of zirconia thermal barrier coatings using sol-gel alumina," *J. Therm. Spray Tech.*, **8**(2), 229-234 (1999).
[25] M. Vippola, J. Vuorinen, P. Vuoristo, T. Lepisto and T. Mantyla, "Thermal analysis of plasma sprayed oxide coatings sealed with aluminum phosphate," *J. Euro. Ceram. Soc*., **22**, 1937-1946 (2002).

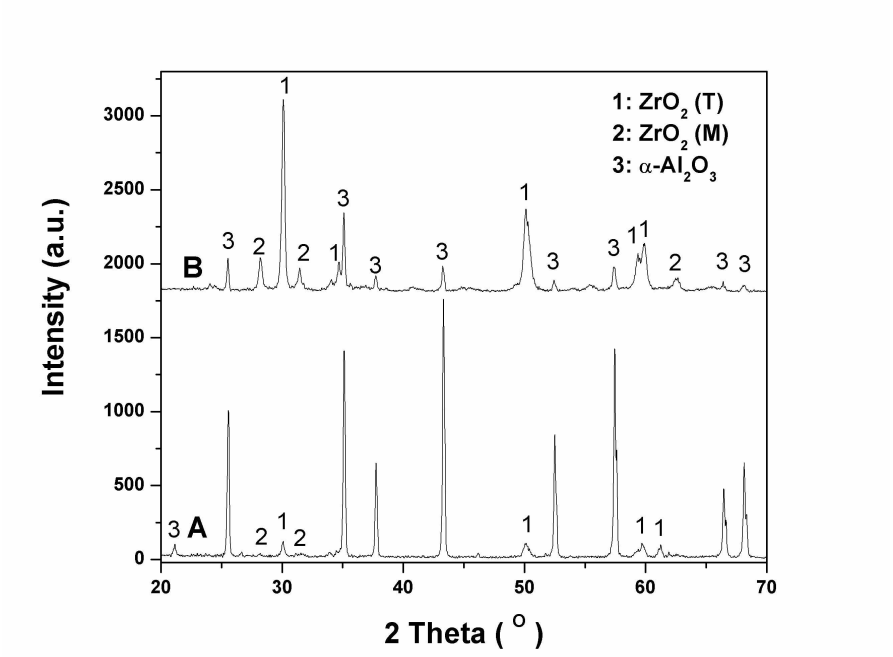

Fig.1 XRD patterns taken from the surface of the YSZ coating with 58 *mm* Al_2O_3 overlay after 10 h of hot corrosion testing at 950°C. (Pattern A: after corrosion testing, Pattern B, after a part of Al_2O_3 overlay was removed)

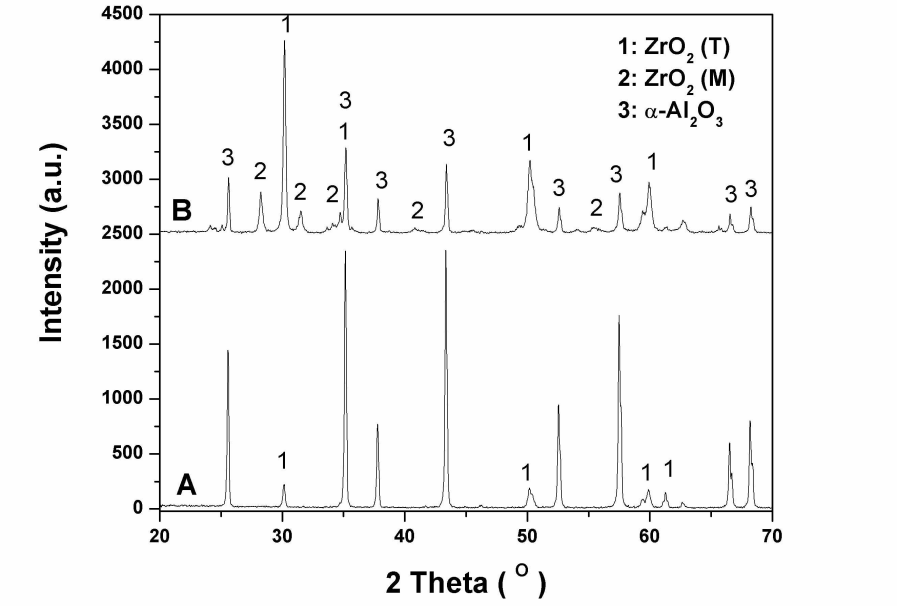

Fig.2 XRD patterns taken from the surface of composite YSZ/Al_2O_3 coating after post annealing at 1200 ^oC (Pattern A) and followed by corrosion testing (Pattern B).

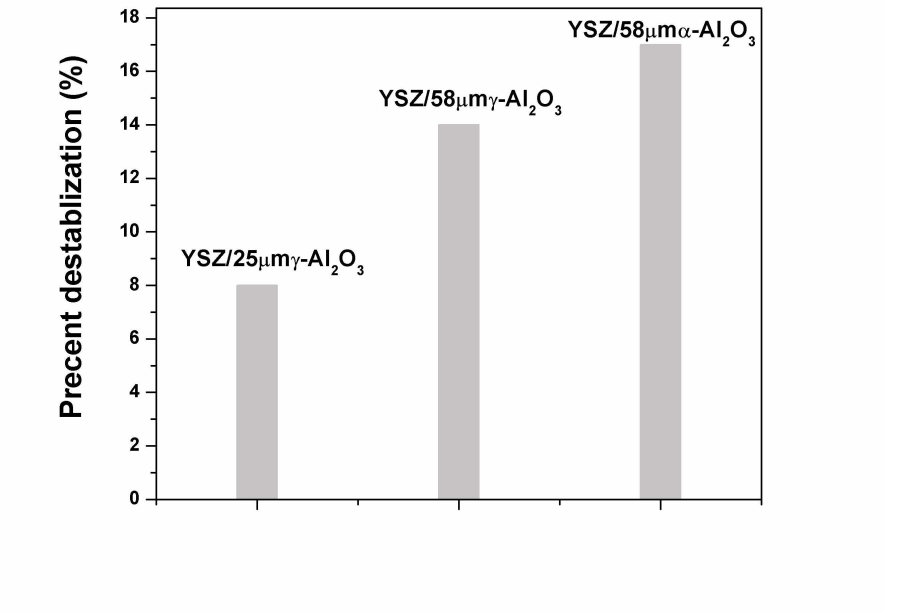

Fig.3 Destabilization fraction of zirconia in the YSZ layer with different Al_2O_3 overlay.

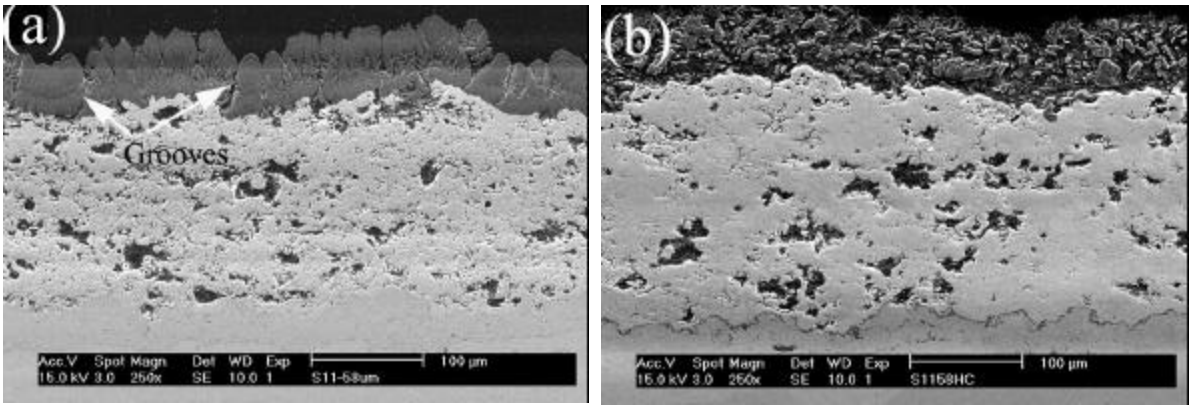

Fig.4 Cross-section SEM images of YSZ with γ-Al_2O_3 overlay before (a) and after exposure to the molten salt (b).

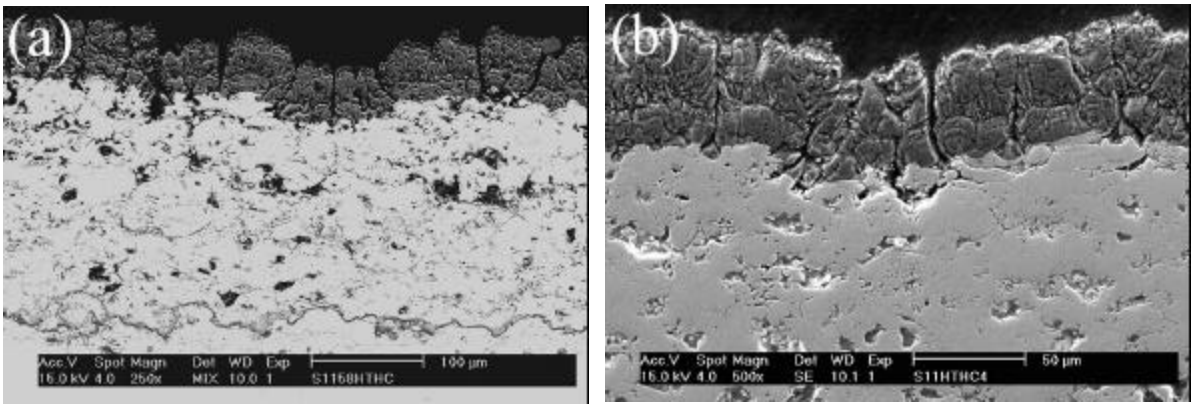

Fig.6 SEM cross-section images of YSZ with 58 *mm* γ-Al_2O_3 overlay after post annealing at 1200^{o}C in air (a) and followed by exposure to the molten salt (b).

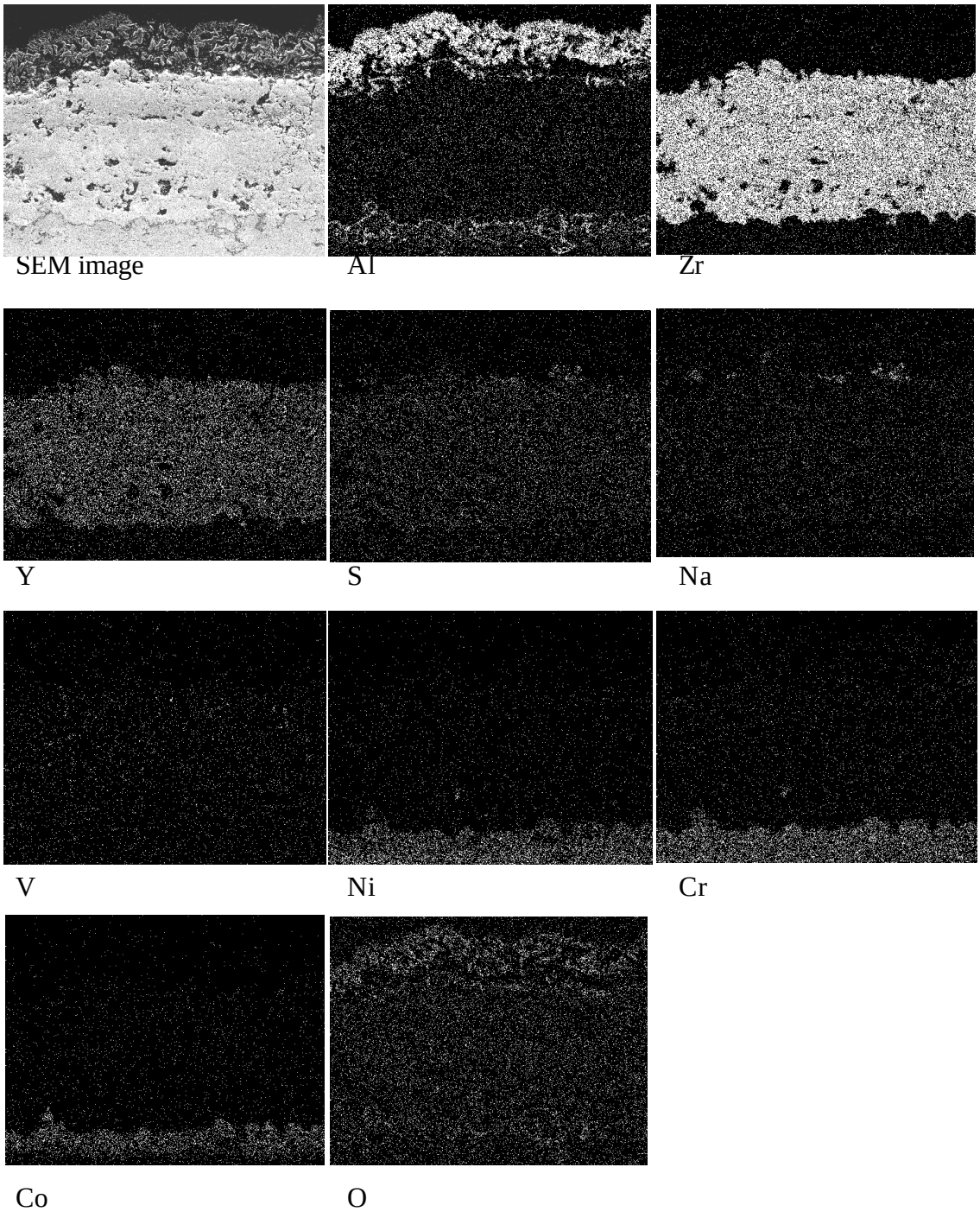

Fig.5 EDS maps of the cross-section of TBC coating after 10 h of hot corrosion testing.

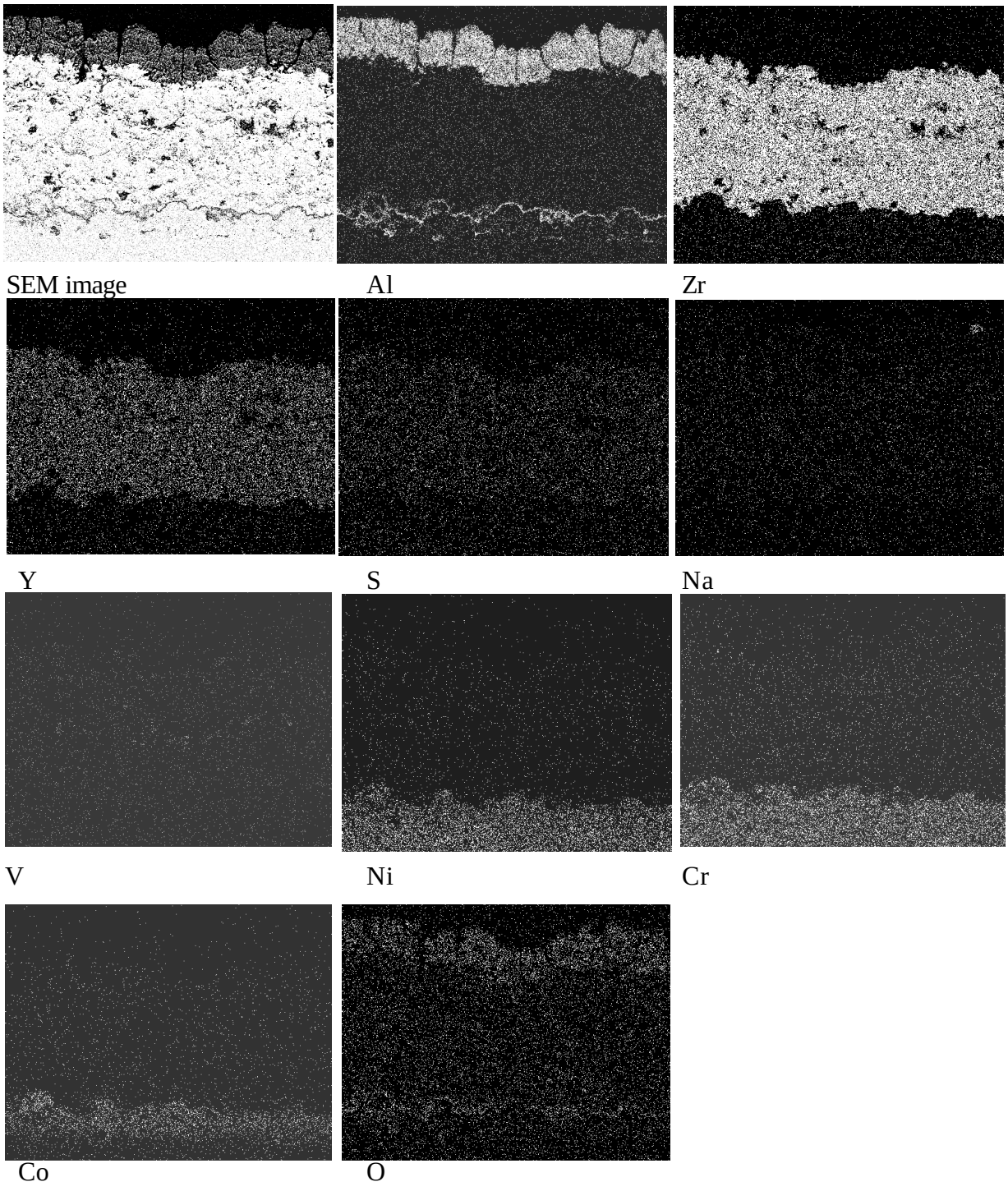

Fig.7 EDS maps of the cross-section of YSZ coating with post annealed Al_2O_3 overlay after 10 h of hot corrosion testing